World Journal of Chemical Education, 2021, Vol. 9, No. 4, 144-151
Available online at http://pubs.sciepub.com/wjce/9/4/7
Published by Science and Education Publishing
DOI:10.12691/wjce-9-4-7

Low-cost Spectroscopy: Experiments in Various Spectral Ranges

Patrick Gräb[1], Ekkehard Geidel[1,*], Hans-Christian Schmitt[2]

[1]Didactics of Chemistry, Julius-Maximilians-Universität Würzburg, 97074 Würzburg, Germany
[2]Institute of Physical and Theoretical Chemistry, Julius-Maximilians-Universität Würzburg, 97074 Würzburg, Germany
*Corresponding author: ekkehard.geidel@uni-wuerzburg.de

Received October 11, 2021; Revised November 12, 2021; Accepted November 28, 2021

Abstract Teaching the basic principles of molecular spectroscopic techniques on an experimental basis is often a particular challenge due to the relatively high cost of the required experimental equipment. The present contribution therefore offers an experimentally-based introduction into the field of spectroscopy using low-cost devices for practical courses at undergraduate level and for chemistry lessons in high schools. Using low-cost devices are also useful for schools in developing countries or poorly-funded school systems. Several experiments, specifically tailored for chemistry lessons, are developed, aiming to provide a close relation to the everyday life experience of students. Initially, a simple spectrometer working within the visible range of light is constructed by the student themselves. This low-cost dispersive spectrometer is employed for quantitative food analyses. In a second step, an introduction to spectroscopy in the near-infrared range is given using an example based on the identification of plastics. On this basis, a model experiment using a self-constructed apparatus for plastic waste separation in miniature was developed. Finally, experiments in the mid-infrared range are presented. They introduce into the functionality of a Michelson interferometer and demonstrate the use of low-cost carbon dioxide sensors. Using this strategy, students gain easier access to an understanding of radiation-matter interaction.

Keywords: *low-cost spectrometer, plastic waste separation in miniature, Michelson interferometer, CO_2 sensor*

Cite This Article: Patrick Gräb, Ekkehard Geidel, and Hans-Christian Schmitt, "Low-cost Spectroscopy: Experiments in Various Spectral Ranges." *World Journal of Chemical Education*, vol. 9, no. 4 (2021): 144-151. doi: 10.12691/wjce-9-4-7.

1. Introduction

Molecular spectroscopy involves the interaction of electromagnetic radiation with matter in order to obtain spectra from which structural and/or quantitative information can be deduced. The traditional procedure to introduce students to the general principles of molecular spectroscopy in lectures and hands-on physical chemistry courses is to follow the electromagnetic radiation systematically in order of increasing frequency in a deductive way. Each energy region corresponds to a different type of molecular process. This strategy may be successful if the previous knowledge of the learners about the quantization of energy levels of matter is more advanced.

An alternative strategy – if the pre-existing knowledge of the learners is less advanced – is to introduce the electromagnetic spectrum and the origin of transitions phenomenologically, with experiments in an inductive manner. Following this strategy, it is possible to start with the technique of UV/Vis spectroscopy. This has two advantages:

(i) The technical setup of an UV/Vis spectrometer is – compared to most other devices – relatively simple. This allows the learners to explore the functionality of each optical component with the help of suited experiments as a preliminary step [1]. Thereby, several low-cost or do-it-yourself devices have been described in the literature [1,2,3,4]. This makes their cost-effective use in hands-on courses and schools feasible.

(ii) Many obvious experiments related to the visible region of radiation (wavelength range 380-780 nm) exist in order to connect the everyday life experience of learners with chemistry-related topics [5]. This type of context-based learning is known to raise interest and emotional valence when dealing with chemical or interdisciplinary scientific problems. In this contribution, experiments for quantitative food analyses were chosen as typical examples.

In a subsequent step, the crossover to the near-infrared range (NIR) can be carried out without fundamental changes in the experimental setup. Of course, special light sources and detectors suited for the NIR range (780-2500 nm) are necessary. Near-infrared spectroscopy is based on the absorption of radiation, which excites molecular overtone and combination modes. Although NIR spectroscopy is not a particularly sensitive technique, it can be very useful in probing bulk materials with little or no sample preparation. Using a model experiment for

waste separation during recycling processes, a typical application of this technique is demonstrated.

Finally, spectroscopy in the mid-infrared range is introduced by experiments demonstrating the functionality of a Michelson interferometer. The experiments include the wavelength determination of a monochromatic light source and the determination of the thermal expansion coefficient of aluminum. With this basic knowledge, the students should be able to understand the functionality of conventional Fourier-transform infrared (FTIR) spectrometers and be able to use them in further university practical courses. However, these spectrometers are rarely available in schools. Therefore, experiments for use in high school chemistry lessons were developed using a nondispersive infrared (NDIR) CO_2 sensor to introduce learners to vibrational excitations. The sensor was utilized in studies of the alcoholic fermentation process and photosynthesis.

2. Experiments in the UV/Vis Range

The techniques of UV/Vis spectroscopy exploit the phenomenon in which radiation in this range of the electromagnetic spectrum (wavelength range 100-780 nm) leads to electronic transitions of atoms and molecules. Such transitions provide limited information on molecular structures, but one of the main applications is in the field of quantitative analyses. For these quantitative analyses, the key equation relating the recorded absorbance to the concentration of the analyte of interest is the Lambert-Beer-Bouguer law [5]. Using this equation, UV/Vis spectroscopy is one of the mostly used routine techniques in quantitative analyses.

2.1. Experimental Setup

To provide initial insight into the functionality of the individual spectrometer components, a dispersive visible-light spectrometer can be constructed by the students. Therefore, a white light LED serves as light source and a digital camera as detector. A small piece of diffraction grating foil attached to the camera operates as dispersive element. The slit is made of two razor blades, which were fitted between the cuvette holder for standard 1 cm cuvettes and the detector. The entire optical setup is stored in a box printed by a 3D printer, as shown in Figure 1. The box has a removable lid allowing students at any time to observe the arrangement of the optical components and of the beam path. The spectrometer is controlled by a Raspberry Pi connected wirelessly to a tablet equipped with the self-programmed control software *Lambda*, which is freely available online [6]. Because the camera records the light intensities at all wavelengths simultaneously, the spectrometer is able to record a visible-light spectrum within several seconds. In the next step, the constructed spectrometer was used for quantitative analyses of proteins and carbohydrates.

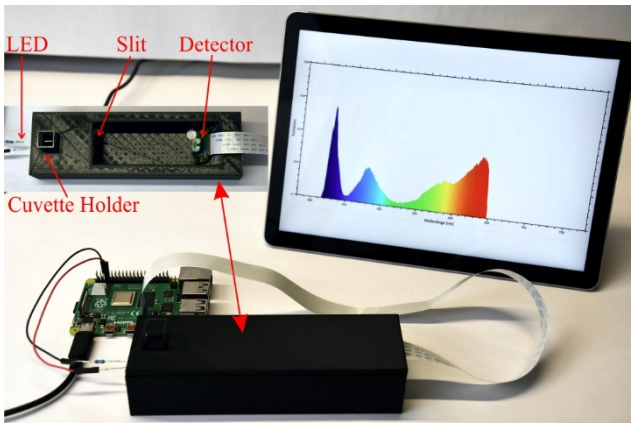

Figure 1. Low-cost spectrometer setup connected via a Raspberry Pi

2.2. Protein Analyses in Foods

Proteins are essential parts of organisms. Animals and humans must consume food containing proteins to ingest essential amino acids. Among the protein sources used in human nutrition are eggs or, alternatively, increasingly popular protein shakes. With respect to a healthy diet, this leads to the context-oriented question:

"*How many eggs have / how much protein shake has to be consumed to obtain the daily requirement of protein for an adult (0.8 g/kg)?*"

The answer to this question can be determined using the spectrometer setup described above. In this regard, the focus was set on casein and ovalbumin as the main protein components in the studied foods. The determination of protein concentrations was determined indirectly using a biuret test, i.e., via the formation of colored biuret protein-copper complexes in alkaline solution. The intensity of the color, and hence the absorption at 540 nm, is directly proportional to the protein concentration, according to the Lambert-Beer-Bouguer law [7]. This simplifies the assay to the evaluation of the results at a single wavelength.

Initially, the wavelength-dependent attenuation coefficients of the copper complexes of casein and ovalbumin were determined with a dilution series of 10 solutions in the concentration range 0.005 – 0.05 g/ml. To each 0.75 ml of the solutions with known protein concentrations, 3 ml biuret reagent (reagent preparation see, e.g. [7]) was added. Instead of ovalbumin, the well-known reference probe bovine serum albumin (BSA) was used [8]. With these solutions, the absorbances at a wavelength of $\lambda = 540$ nm were recorded and from the slopes of linear calibration curves attenuation coefficients were determined to be $\varepsilon_\lambda = 4.0891$ ml g^{-1} cm^{-1} for the casein complex and $\varepsilon_\lambda = 6.2782$ ml g^{-1} cm^{-1} for the BSA complex.

In a second step, samples were prepared by separating the egg white from the yolk using hen's eggs. The masses and volumes were determined, and 150 ml of a 1.713 M sodium chloride solution was added. For the protein shakes, 0.5 g of the powders were dissolved in 22.5 ml distilled water and 2.5 ml of 1 M sodium hydroxide solution was added. With these probe solutions, after

adding the biuret reagent the absorbances at $\lambda = 540$ nm were recorded, respectively. The results obtained by this assay are listed in Table 1 in comparison with values known from the literature [9] or, for protein shakes, those provided by the manufacturer specifications.

Table 1. Comparison of results for quantitative protein analyses with values from the literature [9] and manufacturer specifications

Sample	E_{450}	ρ [g/ml]	$\rho_{manu.}$ [g/ml]
Egg White	0.198	0.0212	0.0206
Egg Yolk	0.954	0.1416	0.094
Protein Shake "Premier Protein"	0.215	0.0161	0.0148
Protein Shake "fitmeals"	0.220	0.0173	0.0153
Protein Shake "Champ"	0.194	0.0109	0.0172

As can be seen from Table 1, the results are acceptable for practical courses. In the case of egg yolk, the outcome shows a relatively large deviation from the expected value. This may be due to turbidity effects disturbing the measurement of the absorbance in this case. Alternatively, the reason for the large deviation may be the high protein concentration observed for egg yolk, which is outside the range of the linear calibration curve.

To answer the question above, we assume an adult with a body weight of 70 kg and a daily protein requirement of 0.8 g/kg. That requires a daily protein consumption of 56 g. To achieve this, about seven hen's eggs (egg white plus egg yolk with 8.55 g protein content per egg) must be eaten per day. Alternatively, three glasses of protein shake, each containing 25 g powder (i.e., 20 g protein) gives the same result. However, the latter variant is probably more pleasant for the consumer.

2.3. Carbohydrate Analyses in Foods

In a second experiment connected to everyday life experiences, the presented low-cost spectrometer can used for quantitative carbohydrate analyses in foods. Carbohydrates play an important role as a source of energy for organisms. In particular, glucose is a nearly universal and accessible source of energy. However, consumption of too much sugar is considered to be a health risk. Therefore, several countries, such as UK, Mexico, and Ireland, have introduced sugar taxes to reduce the consumption. For example, in 2018, Ireland raised a "*sugar sweetened drinks tax*" of 0.16 €/l for drinks with sugar content of 5-8 g/100 ml and of 0.24 €/l for drinks with sugar content more than 8 g/100 ml [10]. This example can be taken as an occasion for the following context-oriented question:

"*What price increase must be expected for lemonade and cola if a sugar tax according to the Irish example is introduced?*"

A suitable method for the quantitative determination of reducing sugar in foods is the reaction with 3,5-dinitrosalicylic acid (DNSA) to form the yellow 3-amino-5-nitrosalicylic acid. The color intensity depends on the concentration of reducing sugar and the amount of sugar can again be determined photometrically.

The experimental procedure, as already described by Harrison et al. [11], was adapted for the application to lemonade and cola drinks. First, 1 g of DNSA was diluted by heating in 20 ml sodium hydroxide solution (c = 2 mol/l) and then a solution of 30 g potassium tartrate diluted in 50 ml distilled water was added. Finally, the solution was diluted to 100 ml with water. Using this solution, the attenuation coefficient of glucose was determined with 10 glucose solutions in the concentration range 0.2 – 2.0 mg/ml at $\lambda = 540$ nm to be $\varepsilon_\lambda = 0.4004$ ml mg^{-1} cm^{-1}.

Most foods do not only contain reducing sugars. To observe the total amount of sugar in foods, the non-reducing sugars must be hydrolyzed first. Thus, 5 ml samples of the two beverages (lemonade and cola) were heated with 10 ml sulfuric acid (c = 2 mol/l) for 20 minutes with stirring in a water bath. After neutralization with sodium hydroxide, the solution was filled up with distilled water to 100 ml. A 10 ml sample from this solution was filled up again with distilled water to 100 ml. The detection of sugar was then carried out photometrically with these solutions using the regression line observed for the dilution series of glucose.

The results are summarized in Table 2 together with the corresponding manufacturer specifications. As can be seen, the deviations are still acceptable in the context of an educational experiment. Even higher sugar content was observed using the same procedure for solid foods (77 g/ 100 g sugar in jam, 94 g/ 100 g sugar in honey, and 47 g/100 g sugar in chocolate spread).

With respect to the original question, the observed sugar contents in Table 2 mean that the price of the lemonade would increase by 0.16 €/l, whereas the price of cola would increase by 0.24 €/l, if an Ireland-style sugar tax were introduced.

Table 2. Comparison of results for quantitative carbohydrate analyses in soft drinks with manufacturer specifications

Sample	E_{540}	ρ [g/ 100 ml]	$\rho_{manu.}$ [g/ 100 ml]
Lemonade	0.055	6.9	8.1
Cola	0.133	12.7	10.8

3. Spectroscopy in the Near-Infrared

The functionality of a dispersive near-infrared spectrometer is, in principle, the same as for spectrometers in the visible range. However, in most applications, the probe preparation is simplified. Near-infrared spectroscopy is based on molecular overtone and combination vibrations. This technique is widely used for routine analytical applications for substance detection or determination of purity. The technique is applied in diverse fields such as agriculture, materials science, medicine, and astronomy [12].

In some chemistry lab courses the demonstration of the advantages and efficiency of NIR spectroscopy, instead of the theoretical background of the method, is often the focus of interest. This can be achieved with practically-oriented experiments. For example, NIR spectroscopy is widely used in industry for the reliable identification of plastics to ensure proper sorting of plastic waste streams.

This situation can be simulated by a model experiment with a self-constructed apparatus for plastic waste separation in miniature.

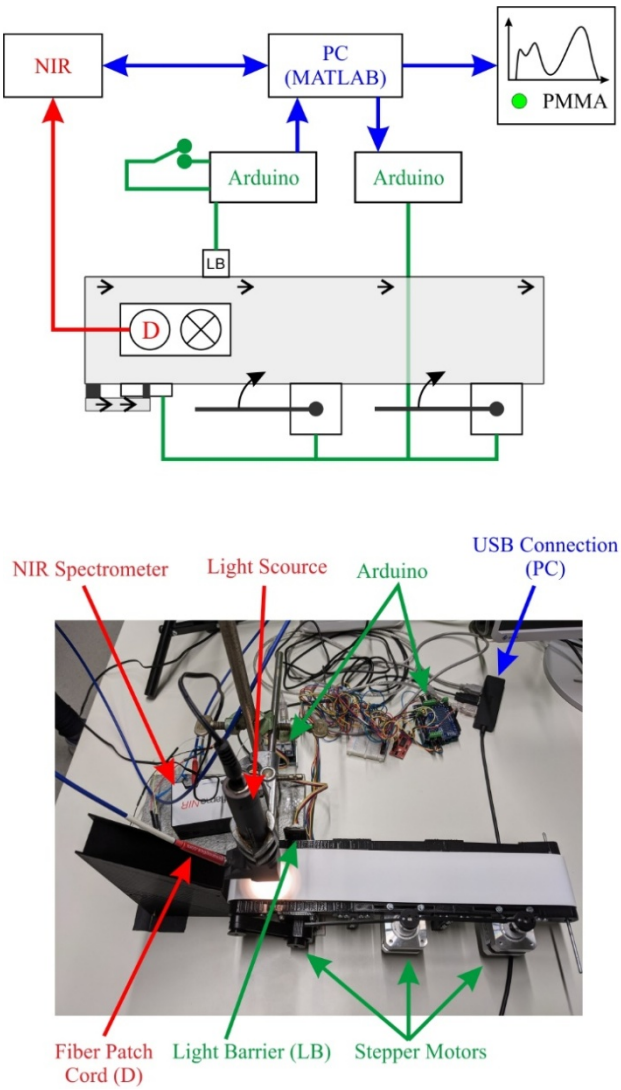

Figure 2. Plastic separation in miniature using NIR diffuse reflectance spectroscopy showing the main components (bottom) and a schematic thereof (top)

The experimental setup (Figure 2) consists of a 30 cm long conveyer belt driven by a stepper motor. Two additional stepper motors move two plastic rods to separate three different kinds of plastics. All stepper motors are connected to Arduino microcontrollers. An additional photoelectric barrier (type VLS3L0X from Seeed) is installed at the top of the conveyer for sample recognition. The heart of the system is a compact *Flame* NIR spectrometer from *OceanOptics* equipped with an optical fiber patch cord and a 45° diffuse reflectance probe with an integrated tungsten halogen light source. The entire system is presented schematically in Figure 2 along with a photograph of its main components.

The entire unit works as follows: initially, the first plastic sample is transported via conveyer to the photoelectric barrier. Then, the conveyer stops and NIR light is sent to and reflected by the plastic sample. Each material has a unique spectrum that is recorded. The kind of plastic is identified by using chemometric models applying the method of principle component analysis (PCA) [13]. For calibration of PCA, a database of NIR spectra of the plastics of interest is necessary. From the analyzed spectrum, the material can then be identified. The separation is realized by activating the plastic rods controlled by a microcontroller. Subsequently, the procedure repeats for the next plastic sample.

The presented setup was tested for several plastics and optimized for the separation of polyethylene (PE), polystyrene (PS), and polymethyl methacrylate (PMMA). For calibration, 10 spectra of each plastic type were recorded in the range 1050-1650 nm. The recorded NIR reflection spectra of PE, PS, and PMMA are presented in Figure 3.

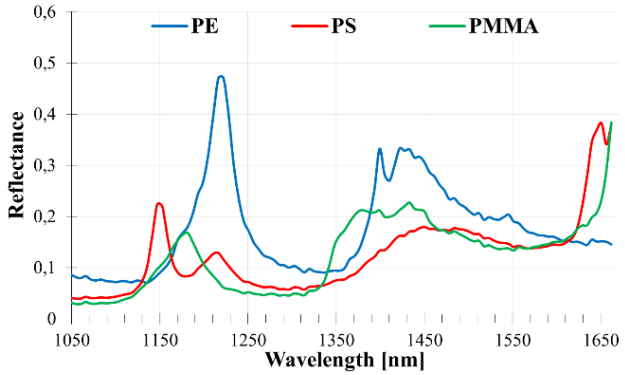

Figure 3. NIR reflection spectra of PE, PS, and PMMA

As can be seen in Figure 3, for all plastics the region 1100-1250 nm is dominated by a strong band assigned to the second overtone of C-H stretching modes [14]. Additionally, a multiple pattern of bands is observed in the range 1300-1450 nm assigned to combination modes. Together these patterns allow identification of the sample by PCA and pattern recognition. Generalizing from this special example it can be concluded that with the help of NIR spectroscopy solutions, most of the common plastics could clearly be identified within seconds.

4. Spectroscopy in the Mid-Infrared

Completing the methods of molecular spectroscopy leads to vibrational spectroscopic techniques, which are suitable for and indeed well established in the determination of molecular structures (cf., e.g. [15,16]). Molecular vibrational spectroscopy deals with all processes of the variation in vibrational motions of molecules induced by radiation. From the three known experimental techniques in the mid-infrared (wavenumber range usually from 4000 to 400 cm^{-1}) – infrared spectroscopy (IR), Raman spectroscopy, and inelastic neutron scattering (INS) – infrared spectroscopy is the most widespread. In many practical courses, small and compact infrared spectrometers are available. In particular, the attenuated total reflection technique (ATR) allows the rapid recording of spectra of solids and liquids without time-consuming sample preparation. In most cases, these ATR-IR spectrometers are considered by students to be “black boxes”, and their inner workings are not discussed.

4.1. The Michelson Interferometer

There are two types of conventional mid-infrared spectrometers: dispersive and interferometric. The Fourier-transform infrared (FTIR) technique has superseded conventional dispersive spectrometers as the predominantly-used spectroscopic instruments because of three well-known advantages, i.e. the multiplex or Fellgett's advantage, the throughput or Jacquinot's advantage, and the wavelength accuracy or Connes' advantage. Therefore, experiments demonstrating the principal functionality of a nondispersive Michelson interferometer are didactically useful to introduce students to the technique of FTIR spectroscopy. Following this concept, a well-suited apparatus is the Michelson interferometer educational kit from *THORLABS* [17] and some of the applications described by the provider [17].

4.1.1. Determining the Wavelength of a Laser

The purpose of practical self-assembly of a Michelson interferometer in lab courses is to explore the function of each component by the students with the help of experiments, following the basic principles of constructionism. The construction can also be combined with the determination of the wavelength of an incident (monochromatic) light, a typical application of an interferometer. The arrangement of the main components of the model interferometer – laser, beam splitter, one fixed and one movable mirror, and a lens – is shown in Figure 4.

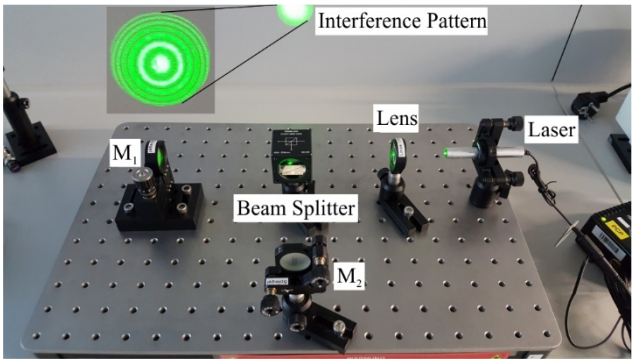

Figure 4. Arrangement of the main components of the model interferometer to determine the wavelength of a green laser

The components are first placed as presented in Figure 4 and the assembly should be carefully adjusted as described in [17]. With this construction, the principles of the fundamental operation of an interferometer can be demonstrated. Half of the source radiation is reflected by the beam splitter, goes to M_2, and back through the beam splitter to the screen. The other half of the radiation is transmitted by the beam splitter, goes to M_1 and back to the beam splitter, where it is reflected and then also reaches the screen. As long as both mirrors have the same distance to the beam splitter, both beams interfere constructively. If M_1 is displaced by a distance of $\lambda/4$, the path of the radiation in that arm is changed by $\lambda/2$, and both beams interfere destructively. A stepwise change of the mirror distance over several micrometers leads then to an observable interference pattern.

For determination of the wavelength, a green light laser (λ = 532 nm) was chosen as radiation source and the screen was substituted by a photodetector (silicon photo diode) for automated evaluation. The voltage was measured by a *GoDirect Voltage Probe* from *Vernier*. Carrying out the experiment, the distance of the moveable mirror from the beam splitter was shortened by Δx = 15 µm in steps of 1 µm. The number of light-dark transitions (number of maxima) in the middle of the interference pattern were counted. The result is presented in Figure 5. From three consecutive measurements an averaged number of N = 56 transitions was observed. Inserting this value into Eq. 1

$$N \cdot \lambda = 2 \cdot \Delta x \text{ or } \lambda = \frac{2 \cdot \Delta x}{N} \quad (1)$$

yields a wavelength of λ = 536 nm for the green laser source. The observed wavelength only differs by approximately 0.75% from the value specified by the provider. In principle, the same setup can be used to observe the emission wavelength of other lasers or monochromatic light-emitting diodes.

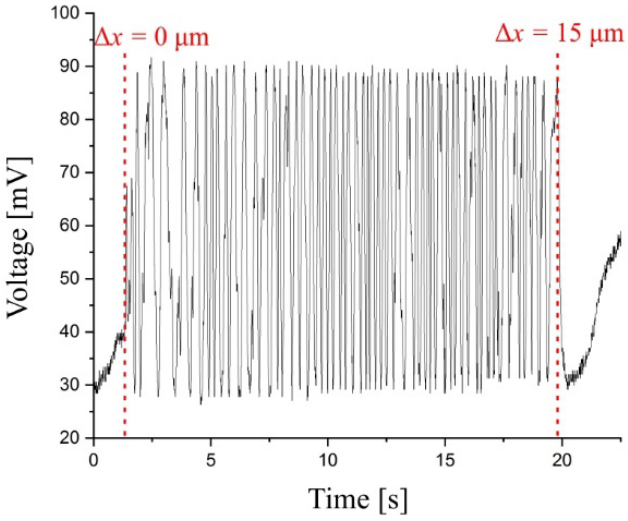

Figure 5. Measured voltages upon changing the mirror displacement up to 15 µm, the number of maxima corresponds to the number of observed light-dark transitions in the interference pattern

4.1.2. Determining the Thermal Expansion Coefficient of an Aluminum Rod

Another impressive application of the Michelson interferometer can be realized when the path length difference between the interferometer arms is caused by thermal expansion of a solid. Such an expansion can be examined by substituting the moveable mirror M_1 (Figure 4) with a mirror attached to the expanding solid [17]. When the solid expands through heating, the path length changes, causing changes in the interference pattern as well. The expansion in linear dimension ΔL can initially be estimated by

$$\Delta L = \alpha \cdot L_0 \cdot \Delta T \quad (2)$$

wherein α is the linear expansion coefficient of the material, L_0 the original length of the solid, and ΔT is the temperature change [18]. Combining Eq. 1 and Eq. 2 – i.e., registering ΔL as the path length difference Δx in the interferometer – the thermal expansion coefficient α can be derived by

$$\alpha = \frac{N \cdot \lambda}{2 \cdot L_0 \cdot \Delta T} \quad (3)$$

To determine the linear expansion coefficient of aluminum, an aluminum rod with an original length of L_0 = 9 cm was used. A flexible polyimide foil heater heats the rod while the temperature is taken with a thermocouple inserted into the rod. The green light laser was taken again as the light source. During heating the aluminum rod to ΔT = 12 K, a total of N = 94 transitions were recorded by the detector. Substituting the observed values into Eq. 3 yields a linear expansion coefficient for aluminum of $\alpha_{Al} = 23.15 \cdot 10^{-6}$ K^{-1}. The observed value is very close to the value of $23.1 \cdot 10^{-6}$ K^{-1} known from the literature for aluminum [19]. It can therefore be concluded that a Michelson interferometer allows a precise determination of very small linear expansions in a small temperature range.

With this basic knowledge of interferometry, students should be able to use compact, conventional FTIR spectrometers routinely in university practical courses. However, apparatus such as this is likely unavailable in schools. Low-cost, self-made versions of FTIR spectrometers are thus far unknown, obviously due to their inherent mechanical fragility. Therefore, for special use in chemistry lessons in schools, experiments were developed using a low-cost nondispersive infrared CO_2 sensor.

4.2. Low-cost Carbon Dioxide Sensors

In the ongoing COVID-19 pandemic, measurement of the CO_2 concentration in school classrooms can ensure that acceptable levels of ventilation for the health of students and teachers is maintained. It is widely recognized that the CO_2 concentration is a good indicator of ventilation rates in classrooms. This current situation can be taken as an occasion to introduce students to the principles of nondispersive infrared spectrometry in chemistry lessons in schools.

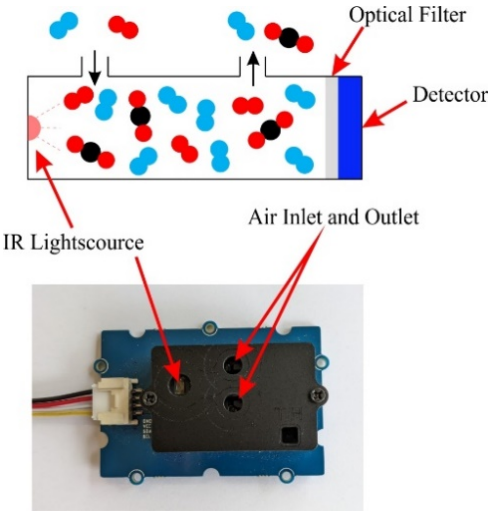

Figure 6. Schematic structure of nondispersive infrared sensor SCD30, adapted from [21]

The most common principles for CO_2 sensors are infrared gas sensors that measure the absorption of a characteristic wavelength in the mid-infrared range. In the setup of the experiments described below a nondispersive, low-cost CO_2 sensor of the type SCD30 (*Seeed*) was used, in combination with an Arduino microcontroller and a coloured LC display. The infrared source installed in the sensor has an emission maximum at 2381 cm^{-1}, close to the absorption maximum of the asymmetric stretching mode of carbon dioxide (ν_{as}(C=O) = 2349 cm^{-1}) [20]. The recorded absorbance at this wavenumber allows measurements of carbon dioxide concentrations in the range 0-10000 ppm with an accuracy of 30 ppm [21]. The schematic structure of the CO_2 sensor is shown in Figure 6.

4.2.1. Carbon Dioxide Release in Alcoholic Fermentation Processes

In anaerobic alcoholic fermentation, sugars are converted into ethanol and carbon dioxide. In the absence of oxygen, yeasts perform this conversion in an enzyme-catalyzed reaction. This can be demonstrated by measuring the CO_2 gas concentration, which is related to the used sugar and yeast concentrations. The simple setup consists of a CO_2 sensor in a closed beaker. The results are presented in Figure 7 for a 20% sucrose solution (bottom) and a 5% yeast solution (top).

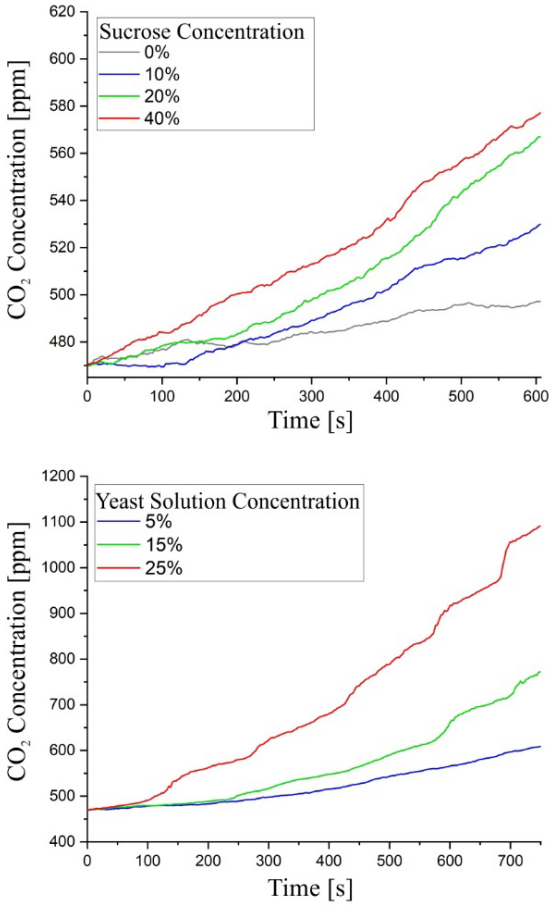

Figure 7. Carbon dioxide release in alcoholic fermentation processes using different sucrose concentrations (top) and different fresh yeast concentrations (bottom)

As expected, the CO_2 concentrations increase in all fermentation processes over the time. The increase is larger for increasing concentrations of sucrose as well as fresh yeast solutions. For sucrose concentration, the dependence of the reaction rate seems to be approximately linear. This observation can be taken as a starting point for further kinetic studies.

4.2.2. Carbon Dioxide Consumption during Photosynthesis

A comparable experimental setup can also be deployed in studies of CO_2 consumption during photosynthesis for fresh spinach leaves under different conditions (Figure 8).

In plant cells, photosynthesis (consuming CO_2) and cell respiration (producing CO_2) proceed simultaneously in an equilibrium which depends on the lighting conditions. To demonstrate this, the reaction vessel depicted in Figure 8 was first illuminated with UV light for 10 minutes. Illumination was then stopped, and the vessel was darkened for 10 minutes using aluminum foil.

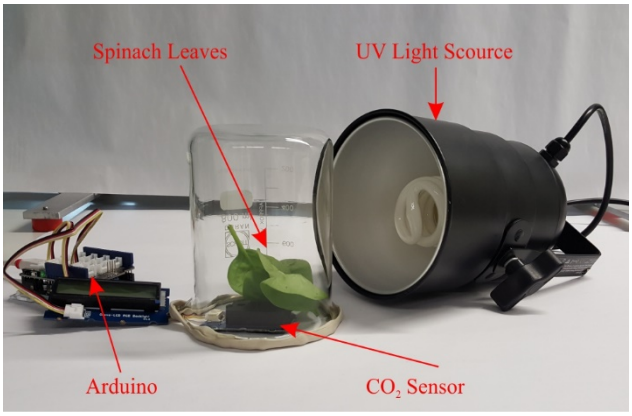

Figure 8. Experimental setup for measuring CO_2 concentrations during photosynthesis and cell respiration

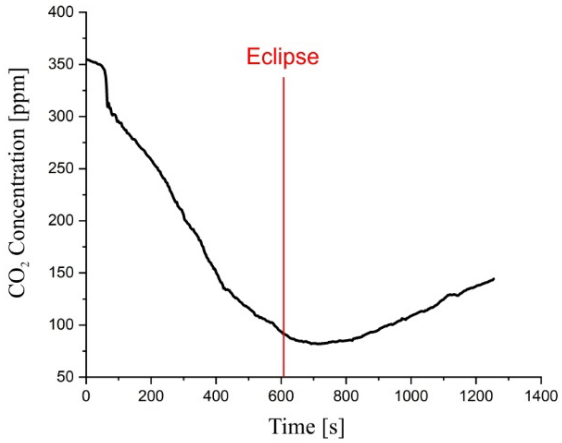

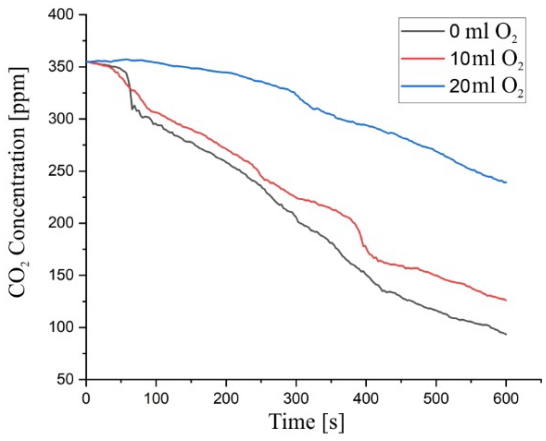

Figure 9. Carbon dioxide concentration before and after darkening the plant's environment (top) and after oxygen enrichment (bottom)

The results of tracking the CO_2 concentration over 20 minutes are presented in Figure 9. As can be seen in Figure 9 (top), a continuous decrease in CO_2 concentration is initially observed for photosynthesis. After 10 minutes (eclipse) the CO_2 concentration again increases due to the dominating cell respiration under these conditions.

Moreover, a third process can be observed indirectly if – before the UV illumination – different amounts of oxygen gas are added (Figure 9, bottom). In this case, a smaller decrease of CO_2 concentrations is observed. Obviously, the plant produces carbon dioxide in a parallel reaction in an oxygenated environment. This process is known as photorespiration, in which oxygen is consumed and carbon dioxide is released by the plant. This can be taken as an indication for two parallel biochemical reactions.

5. Conclusions

In this contribution, we present phenomenological and experiment-based methods to access the basic principles of the interaction of electromagnetic radiation with matter. Experiments were developed with a connection to the everyday life of students using different spectral ranges of molecular spectroscopy (UV/Vis, NIR, and MIR). Of course, the connection of the experiments to everyday life experiences depends on the target group. For chemistry lessons in high schools, context-based learning is of particular importance to raise the interest and motivation of learners in chemistry-related topics.

In contrast to traditional, theory-heavy methods of teaching, the introduction described here starts with the self-construction of a low-cost visible-light spectrometer. After having assembled such a spectrometer, learners explore the use of the instrument in practical applications. This low-cost device has the advantage that it can be used in multiple courses with many students. The results achieved with the spectrometer for quantitative analyses of proteins and carbohydrates in foods are satisfactory for this purpose. The quantitative analyses experiments have open questions and a context-based motivation trigger for learners. Thereby, it was possible to link chemical applications with everyday life.

Subsequently, a model experiment is presented to introduce learners to the field of NIR spectroscopy. As an application of NIR spectroscopy, this technique is used – in combination with chemometric models – for the identification of different types of plastics. A small plastic sorting system controlled by an Arduino microcontroller is constructed for use as a model for typical industrial applications.

The preferred method in the field of vibrational spectroscopy is the Fourier-transform infrared technique. Therefore, experiments demonstrating the principal functionality of a nondispersive Michelson interferometer are presented. Based on their knowledge of interferometry, students should be able to use compact, conventional Fourier transform infrared spectrometers routinely. However, spectrometers such as these are rare in high schools. Hence, for application in schools, experiments were developed using a low-cost nondispersive infrared CO_2 sensor. Experiments measuring the changes of CO_2

gas concentration in alcoholic fermentation and photosynthesis processes demonstrate the simple but valuable applications of such sensors.

In summary, the chosen inductive method appears to provide an easier access overall to spectroscopic techniques in chemical education. A survey conducted among 32 students using questionnaires on a six-level Likert scale (items from (1) strongly disagree to (6) strongly agree) yielded the following assessments. With a statistical mean of 5.3 ($\sigma = 1.2$) the students voted that a concrete reference to everyday life is helpful to introduce to physico-chemical methods. Teaching of physico-chemical contents using low-cost devices was evaluated to be meaningful by a statistical mean of 5.5 ($\sigma = 0.6$).

Acknowledgements

The authors thankfully acknowledge THORLABS GmbH for fruitful collaboration. Max and Jonas Hofmann are acknowledged for testing most of the experiments in laboratory courses.

This publication was funded by the German Research Foundation (DFG) and the Julius-Maximilians-Universität Würzburg via the funding program Open Access Publishing.

References

[1] Schairer, P., Wagner, S., and Geidel, E., "An Experimental Introduction to Basic Principles of the Interaction of Electromagnetic Radiation with Matter," *World Journal of Chemical Education*, 6(1), 29-35, Jan. 2018.

[2] Grasse, E. K., Torcasio, M. H., and Smith, A. W., "Teaching UV-Vis Spectroscopy with a 3D-Printable Smartphone Spectrophotometer," *Journal of Chemical Education*, 93(1), 146-151, Jan. 2016.

[3] Bougot-Robin, K., Paget, J., Atkins, S. C., and Edel, J. B., "Optimization and Design of an Absorbance Spectrometer Controlled Using a Raspberry Pi To Improve Analytical Skills," *Journal of Chemical Education*, 93(7), 1232-1240, Jul. 2016.

[4] Gräb, P., Kahre, M., Woßmann, P., and Geidel, E., "Selbst messen und Versuche digital auswerten," *Nachrichten aus der Chemie*, 69(7-8), 14-17, 2021.

[5] Gräb, P. and Geidel, E., "Spectroscopic Studies of Food Colorings," *World Journal of Chemical Education*, 7(2), 136-144, Apr. 2019.

[6] Gräb, P., Kahre, M., and Woßmann, P., "Low-Cost Messgeräte," 2021. [Online]. Available: https://www.chemie.uni-wuerzburg.de/didaktik/lehrende/low-cost-messgeraete/. [Accessed: 05-Mar-2021].

[7] Lottspeich, F. and Engels, J. W., *Bioanalytics: Analytical Methods and Concepts in Biochemistry and Molecular Biology*, John Wiley & Sons, 2018.

[8] Sapan, C. V., Lundblad, R. L., and Price, N. C., "Colorimetric protein assay techniques," *Biotechnology and Applied Biochemistry*, 29(2), 99-108, 1999.

[9] Matissek, R. and Baltes, W., *Lebensmittelchemie*, 8th ed., Berlin [u.a.], Springer Spektrum, 2016.

[10] Studdert, D. M., Flanders, J., and Mello, M. M., "Searching for Public Health Law's Sweet Spot: The Regulation of Sugar-Sweetened Beverages," *PLoS Medicine*, 12(7), Jul. 2015.

[11] Harrison, T., Gros, N., Dolinar, A. K., and Drusany, I. Š., "Spectrometry at school: hands-on experiments," *Science in School*, (14), 42-47, 2010.

[12] Burns, D. A., *Handbook of Near-Infrared Analysis*, 3rd ed., Boca Raton, FL [u.a.], CRC Press [u.a.], 2008.

[13] Wold, S., "Chemometrics; what do we mean with it, and what do we want from it?," *Chemometrics and Intelligent Laboratory Systems*, 30(1), 109-115, Nov. 1995.

[14] Eisenreich, N. and Rohe, T., "Infrared Spectroscopy in Analysis of Plastics Recycling," *Encyclopedia of Analytical Chemistry*. John Wiley & Sons, 2006.

[15] Colthup, N., Daly, L., and Wiberley, S., *Introduction to Infrared and Raman Spectroscopy*, 3rd ed., New York, Elsevier, 1990.

[16] Karge, H. G. and Geidel, E., "Vibrational Spectroscopy," in *Molecular Sieves - Science and Technology*, Berlin, Springer Verlag, 2004, 1-200.

[17] Thorlabs, "Michelson-Interferometer-Kit," 2021. [Online]. Available: https://www.thorlabs.com/newgrouppage9.cfm?objectgroup_id=10107. [Accessed: 01-Jun-2021].

[18] Halliday, D., Resnick, R., and Walker, J., *Halliday Physik für natur- und ingenieurwissenschaftliche Studiengänge*, 3rd ed., Weinheim, Wiley-VCH, 2020.

[19] Lide, D. R., *CRC Handbook of Chemistry and Physics*, 87th ed., Boca Raton [u.a.], Taylor & Francis, 2006.

[20] Weidlein, J., Müller, U., and Dehnicke, K., *Schwingungsspektroskopie: Eine Einführung*, 2nd ed., Stuttgart, Georg Thieme Verlag, 1988.

[21] seeed, "Grove - CO2 & Temperature & Humidity Sensor for Arduino (SCD30) - 3-in-1," 2021. [Online]. Available: https://www.seeedstudio.com/Grove-CO2-Temperature-Humidity-Sensor-SCD30-p-2911.html. [Accessed: 19-Apr-2021].